Beam-induced heating at low electron fluxes during liquid phase transmission electron microscopy

Birk Fritsch[1], Andreas Hutzler[1], Mingjian Wu[2], Lilian Vogl[3], Michael P.M. Jank[4], Martin März[5] and Erdmann Spiecker[2]

[1]Electron Devices (LEB), Department of Electrical, Electronic and Communication Engineering, Friedrich-Alexander University Erlangen-Nürnberg (FAU), Erlangen, Germany, Erlangen, Bayern, Germany, [2]Institute of Micro- and Nanostructure Research (IMN) & Center for Nanoanalysis and Electron Microscopy (CENEM), Interdisciplinary Center for Nanostructured Films (IZNF), Department of Materials Science and Engineering, Friedrich-Alexander University Erlangen-Nürnberg (FAU), Erlangen, Germany, Erlangen, Bayern, Germany, [3]Institute of Micro- and Nanostructure Research (IMN) & Center for Nanoanalysis and Electron Microscopy (CENEM), Interdisciplinary Center for Nanostructured Films (IZNF), Department of Materials Science and Engineering, Friedrich-Alexander University Erlangen-Nürnberg (FAU), Erlangen, Bayern, Germany, [4]Fraunhofer Institute for Integrated Systems and Device Technology IISB, Erlangen, Germany, Erlangen, Bayern, Germany, [5]Electron Devices (LEB), Department of Electrical, Electronic and Communication Engineering, Friedrich-Alexander University Erlangen-Nürnberg (FAU), Erlangen, Germany, Erlangen, Germany

Especially when investigating heavy metal structures such as gold nanoparticles, secondary electrons increase the effective dose locally (Gupta *et al.*, 2018; Korpanty *et al.*, 2021). This is particularly significant, because gold nanostructures are one of the most frequently analysed material systems in LPTEM. Investigating beam-induced heating on gold nanoparticles is, thus, of utmost importance.

In this contribution, we demonstrate that parallel-beam electron diffraction (PBED) (Niekiel *et al.*, 2017) is applicable for *in situ* monitoring temperature within the irradiated volume during LPTEM by precise evaluation of the thermally-induced expansion of the crystal lattice (Fritsch *et al.*, 2021). Furthermore, we apply this method to show that significant electron beam induced heating can occur in LPTEM even for relatively low electron fluxes.

To demonstrate the capability of local temperature measurement, *in situ* chip-based heating was applied. The measurement principle is sketched in Figure 1(a): 18 nm of gold were sputter-deposited on a Protochips Poseidon Select heating chip and dewetted to obtain gold nanoparticles by using a hot plate at 200°C. To ensure a sufficiently thin layer for collecting diffraction data during TEM, an air-bubble was introduced during chip mounting. The water thickness was determined to 140 nm by the t/λ-method utilizing electron-energy loss spectroscopy (EELS). Data acquisition was performed using an image and probe corrected FEI TITAN Themis³ 80-300 (S)TEM at 300 kV acceleration voltage adjusting an electron flux density of 5 e⁻/Å²s and 1 s acquisition time. After establishing parallel beam illumination by fine-tuning the condenser lens currents (Niekiel *et al.*, 2017) a heating profile was applied.

Selected area electron diffraction patterns (Figure 1(b)) of gold nanoparticles reveal a relative change of the diffraction ring radius with temperature (Figure 1(c)). The temperature change of irradiated particles is obtained (Figure 1(d)) by comparing their lattice parameters with theoretical values of the thermal expansion coefficient of gold (Touloukian, 1970). Data obtained by complementary resistivity-based temperature measurements are in good agreement for the first 220 s of the conducted experiment. After this period of time, the temperature obtained via PBED analysis starts to deviate, emphasizing the

requirement of measuring temperature directly at the spot of observation. One remarkable observation is, that during the cool down period the temperature does not settle again at the starting temperature whilst illuminated by the electron beam.

To access beam-induced heating during LPTEM, the experimental set up was irradiated without external heating for five minutes at low electron flux densities between 0.7 and 3 e⁻/Å²s. The beam was blanked for 10 min prior to every experiment to allow the system to settle again. Exemplary profiles of such an experiment are shown in Figure 2(a). The shaded data range is used for determining the flux-dependent temperature increase. These profiles reveal significant temperature changes even at low electron flux densities (Figure 2(b)). The relative changes of the 220 and 311 diffraction rings are used for thermometry. The large error bar at the lowest electron flux can be attributed to the reduced signal-to-noise ratio. Linear regression reveals an electron flux density-dependent heating of 9.22 KÅ²s⁄e⁻ for our experiments.

The results demonstrate the necessity for an accurate consideration of heating effects when analysing thermal and chemical dynamics during LPTEM. Furthermore, we emphasize that this effect can be utilized for adjusting the local temperature during LPTEM even without dedicated heating holders by fine-tuning the experimental environment as well as the electron flux density.
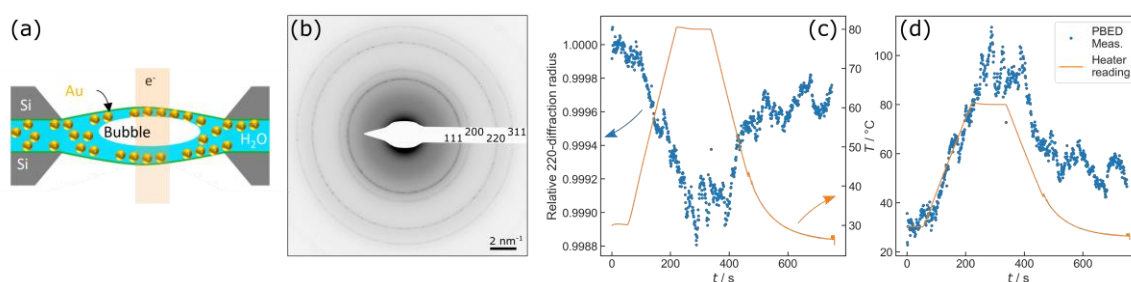

Figure 1. (a) Scheme for acquisition of diffraction data from gold nanoparticles using PBED in LPTEM. (b) Exemplary diffraction pattern acquired for thermometry. (c) Relative change of the radius of the (220) diffraction ring during heating. (d) The obtained temperature measurement within the irradiated area in comparison to the heater reading.
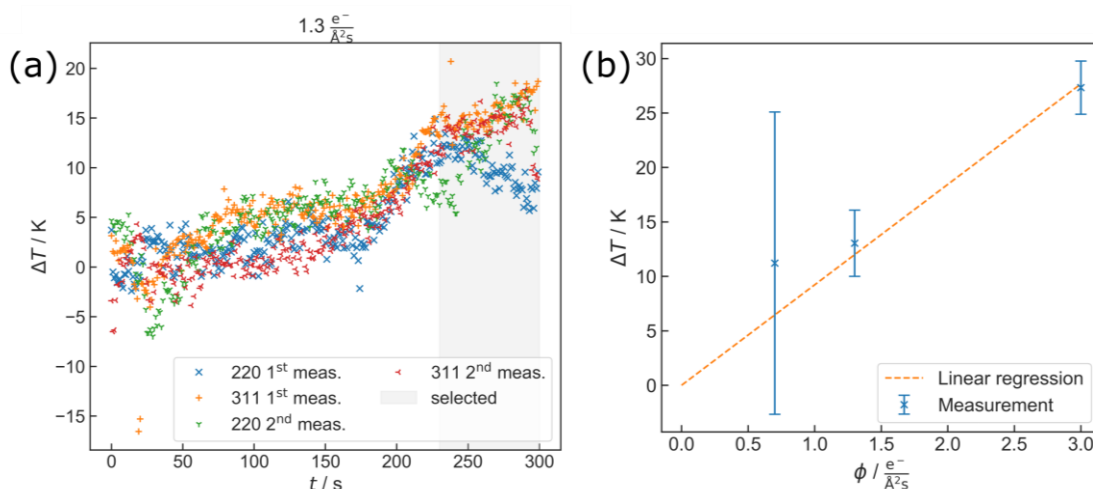

Figure 2. (a) Exemplary in situ temperature profiles during irradiation. (b) A linear increase of beam-induced heating with the electron flux density Φ is demonstrated. The error bars mark the deviation between the 220 and 311 data.

References

Fritsch B, Hutzler A, Wu M, Khadivianazar S, Vogl. Lilian, Jank MPM, März M and Spiecker E (2021) Accessing local electron-beam induced temperature changes during in situ liquid-phase transmission electron microscopy. *Nanoscale Adv.* **3**, 2466-2474.

Gupta T, Schneider NM, Park JH, Steingart D and Ross FM (2018) Spatially dependent dose rate in liquid cell transmission electron microscopy. *Nanoscale* **10**, 7702–7710.

Hsieh T-H, Chen J-Y, Huang C-W and Wu W-W (2016) Observing Growth of Nanostructured ZnO in Liquid. *Chem. Mater.* **28**, 4507–4511.

Hutzler A, Fritsch B, Jank MPM, Branscheid R, Martens RC, Spiecker E and März M (2019) In Situ Liquid Cell TEM Studies on Etching and Growth Mechanisms of Gold Nanoparticles at a Solid–Liquid–Gas Interface. *Adv. Mater. Interfaces* **345**, 1901027.

Hutzler A, Schmutzler T, Jank MPM, Branscheid R, Unruh T, Spiecker E and Frey L (2018) Unravelling the Mechanisms of Gold-Silver Core-Shell Nanostructure Formation by in Situ TEM Using an Advanced Liquid Cell Design. *Nano Lett.* **18**, 7222–7229.

Korpanty J, Parent LR and Gianneschi NC (2021) Enhancing and Mitigating Radiolytic Damage to Soft Matter in Aqueous Phase Liquid-Cell Transmission Electron Microscopy in the Presence of Gold Nanoparticle Sensitizers or Isopropanol Scavengers. *Nano Lett.*, 1141–1149.

Lu Y, Wang K, Chen F-R, Zhang W and Sui ML (2016) Extracting nano-gold from HAuCl4 solution manipulated with electrons. *Phys Chem Chem Phys* **18**, 30079–30085.

Niekiel F, Kraschewski SM, Müller J, Butz B and Spiecker E (2017) Local temperature measurement in TEM by parallel beam electron diffraction. *Ultramicroscopy* **176**, 161–169.

Schneider NM, Norton MM, Mendel BJ, Grogan JM, Ross FM and Bau HH (2014) Electron–Water Interactions and Implications for Liquid Cell Electron Microscopy. *J. Phys. Chem. C* **118**, 22373–22382.

Touloukian YS (ed.) (1970) *Thermophysical properties of matter*: *The TPRC data series ; a comprehensive compilation of data*. New York, NY: IFI/Plenum.